Polymer 49 (2008) 5169–5176

Contents lists available at ScienceDirect

Polymer

journal homepage: www.elsevier.com/locate/polymer

# On the molecular properties of polyaniline: A comprehensive theoretical study

Carlos Alemán [a,*], Carlos A. Ferreira [b], Juan Torras [c], Alvaro Meneguzzi [b], Manel Canales [d], Marco A.S. Rodrigues [b], Jordi Casanovas [e,**]

[a] Departament d'Enginyeria Química, E.T.S. d'Enginyers Industrials de Barcelona, Universitat Politècnica de Catalunya, Diagonal 647, Barcelona E-08028, Spain
[b] Universidade Federal do Rio Grande do Sul – DEMAT, Av. Bento Gonçalves, 9500, setor 4, prédio 74, Cep. 91501-970, Porto Alegre, RS, Brazil
[c] Departament d'Enginyeria Química, EUETII, Universitat Politècnica de Catalunya, Pça Rei 15, Igualada 08700, Spain
[d] Departament de Física I Enginyeria Nuclear, Facultat d'Informàtica,, Universitat Politècnica de Catalunya, Jordi Girona 1-3, Barcelona E-08034, Spain
[e] Departament de Química, Escola Politècnica Superior, Universitat de Lleida, c/Jaume II no. 69, Lleida E-25001, Spain

ARTICLE INFO

*Article history:*
Received 14 August 2008
Received in revised form 8 September 2008
Accepted 8 September 2008
Available online 27 September 2008

*Keywords:*
Polyaniline
Polaron
Conducting polymer

ABSTRACT

A comprehensive study about the molecular and electronic properties of the different forms of polyaniline has been developed using quantum mechanical calculations. Initially the performance of different ab initio and DFT quantum mechanical methods has been evaluated by comparing the results provided for small model compounds containing two repeating units. After this, calculations on the emeraldine base, leucoemeraldine base, pernigraniline base and emeraldine salt (monocationic and dicationic) forms of oligoanilines with *n* repeating units, where *n* ranged from 5 to 13, have been performed using the BH&H/6-31G(d) method, which was found to be a very suitable theoretical procedure. Interestingly, calculations indicate that the distribution in blocks of the repeating units containing amine and imine nitrogen is largely preferred for the emeraldine base form. On the other hand, the molecular structure and band gap of the emeraldine base, leucoemeraldine base and pernigraniline base forms have been rationalized according to their differences in the conjugation of the $C_6H_4$ rings. Calculations on cationic oligoanilines indicate that, when the emeraldine salt form presents a doublet electronic state, the positive charge and the spin density are located in the middle of the chain extending through five consecutive repeating units.



## 1. Introduction

In recent years a large number of quantum mechanical studies have been devoted to study the structural and electronic properties of conducting oligomers and polymers derived from thiophene and pyrrole [1–8]. These investigations have been extremely useful not only to rationalize the experimental observations but also to develop the comprehensive design of new conducting materials by using the knowledge provided by such calculations. In contrast, the number of studies devoted to understand the properties of polyaniline (hereafter denoted PAni) through the application of sophisticated quantum mechanical methods is relatively scarce [9–15] even though the use of this conducting polymer has continued to grow in recent years. The remarkable interest on this material is because of its excellent properties: high chemical and environmental stabilities, remarkable electrical conductivity in the doped state, easy processability and low cost.

In the last decade some theoretical studies have been devoted to study oligoanilines and/or PAni using ab initio and/or Density Functional Theory (DFT) methods [9–15]. In an early study Lim and co-workers used the HF and BLYP methods combined with a 6-31G basis set to examine the geometric and electronic properties of small neutral aniline oligomers [12]. More recently, Foreman and Monkman [13] investigated the influence of intermolecular bonds with sulfonic acid on the molecular and electronic structures of simple PAni models. Calculations at the B3LYP/6-311++G(2d,2p) level showed that the hydrogen bond between the amine and sulfonic acid groups increases the ability of the phenyl–nitrogen–phenyl backbone to transfer electron density. On the other hand, the doping of PAni by acid–base chemistry was studied using DFT calculations (LSDA, PBE and PBE0 functionals) with periodic boundary conditions and the 6-31G(d,p) basis set [14]. The structural and spectroscopical predictions reported in such work for both the polaron and bipolaron agreed quite well with experimental data. In a very recent study, Hou and co-workers [15] analyzed the electronic structure of oligoanilines after doping with

* Corresponding author.
** Corresponding author.
*E-mail addresses:* carlos.aleman@upc.edu (C. Alemán), jcasanovas@quimica.udl.es (J. Casanovas).

0032-3861/$ – see front matter © 2008 Elsevier Ltd. All rights reserved.
doi:10.1016/j.polymer.2008.09.023

hydrochloric acid and camphorsulfonic acid using a DFT method with generalized gradient approximation and PBE functional combined with the 6-31G(d) basis set. Results indicated that the latter dopant induces more charge transfer than the former one explaining the differences found in the electrical conductivity of PAni when is doped with hydrochloric acid or camphorsulfonic acid.

A detailed inspection of the theoretical studies described above [9–15] reveals that these results cannot be compared directly, and therefore, only general and qualitative trends can be extracted. This should be mainly attributed to four reasons: (i) different approaches, levels of theory, or both were employed for the calculations, that is, ab initio or DFT methods, basis sets, etc; (ii) the studies were performed on oligoanilines of different lengths, usually involving a very reduced number of repeating units; (iii) different redox states were considered in each study, that is, doped or undoped states, and within each one different forms; and (iv) the aim was completely different for each study, that is, analyses of the results were focused on the molecular geometry, electronic structure, spectroscopical properties or the doping process by itself. Although some systematic studies involving PAni have been reported, no attempt has been made to investigate the properties of its different doped and undoped forms using identical and comparable conditions. Thus, a complete description of the microscopic peculiarities, *i.e.* molecular and electronic structures that control the properties of this important conducting polymer has not been achieved yet. This is the first motivation of the present study. Furthermore, computational power has increased significantly in the last few years, quantum mechanical calculations on conducting polymers using a reasonably large number of repeating units being currently possible. Accordingly, the prediction of the above-mentioned properties on large conjugated oligomers is the second motivation of our study. In this work we present a comprehensive investigation that involves different aspects of the molecular and electronic structures of PAni in their neutral and oxidized forms. Calculations have been performed considering oligoanilines formed by a number of repeating units ranging from 5 to 13, results being extrapolated to infinite polymer chains.

Specifically, our approach is outlined as follows. In the next section we describe the molecular systems and the theoretical procedures employed for the development of this study. After this, we present a systematic investigation devoted to identify a theoretical procedure able to describe medium and large oligoanilines at a reasonable computational cost. For this purpose we considered a small model molecule in its neutral, cationic and dicationic (both singlet and triplet) states, these systems being investigated using two ab initio (HF and MP2) and two DFT (B3LYP and BH&H) methods combined with four basis sets (6-31G(d), 6-31+G(d,p), cc-pVDZ and cc-pVTZ). Next, the molecular and electronic structures of neutral and oxidized forms of PAni are discussed and compared. In order to achieve this, calculations on oligomers with a growing number of repeating units were performed using the selected theoretical procedure. Specifically, discussion refers to the geometrical parameters, the twisting of the chain backbone, the stability of the different forms (if proceed), the distribution of $C_6H_4$ rings with benzenoid-like and quinoid-like structures through the chain, the $\pi$–$\pi^*$ lowest transition energy ($\varepsilon_g$) and the distribution of charges and spin densities in charged systems. Finally, the last section is devoted to summarize the main conclusions of this work.

## 2. Methods

### 2.1. Molecular systems

The structure of PAni consists of a series of $C_6H_4$–N repeating units, where the nitrogen exists in either an amine or imine environment. Thus, PAni can be found as emeraldine base (EB; half oxidized form), leucoemeraldine base (LB; fully reduced form) or pernigraniline base (PNB; fully oxidized form) depending on the degree of oxidation of the nitrogen atoms (Scheme 1). The conducting emeraldine salt (ES) form can be obtained by oxidative doping of LB or by protonation of EB, *i.e.* doping with protonic acids (Scheme 2).

In this work we examined the molecular and electronic structures of oligomers involving the EB, LB, PNB and ES forms of PAni. These oligomers have been denoted EB-*n*, LB-*n*, PNB-*n* and ES-*n*, respectively, where *n* refers to the number of $C_6H_4$ rings independently of their benzonoid- or quinoid-like structure. ES-*n* oligomers have been calculated in both cationic and dicationic forms, which have been identified as ES-$n^+$ and ES-$n^{2+}$, respectively. All the calculated oligomers were blocked at the ends by nitrogens in amine or imine forms depending on the structure considered for PAni.

### 2.2. Theoretical procedures

All the calculations were performed using the Gaussian 03 computer program [16]. In order to ascertain the performance of different theoretical methods, complete geometry optimizations of LB-2 and PNB-2, ES-$2^+$ and ES-$2^{2+}$ were performed using the HF, MP2 [17], B3LYP [18,19] and BH&H [18] methods combined with the 6-31G(d) [20], 6-31+G(d,p) [21], cc-pVDZ [22] and cc-pVTZ [23] basis sets. It should be noted that the BH&H functional has been included in this study because it was recently found to describe satisfactorily the $\pi$-aromatic systems, particularly the interaction between $\pi$-clouds [24]. Calculations on LB-2 and PNB-2 were performed using the restricted formalism of these theoretical methods, while the unrestricted formalism was employed for ES-$2^+$ (doublet electronic state) and ES-$2^{2+}$. The latter was computed in both the singlet and triplet electronic states, hereafter denoted ES-$2^{2+}$(S) and ES-$2^{2+}$(T), respectively. These states allow describe the fact that an isolated oligomer carrying two positive charges can form either a bipolaron or a pair of polarons [3,25].

On the other hand, calculations on EB-*n*, LB-*n* and PNB-*n* with *n* ranging from 5 to 11 were performed using the restricted formalism of the BH&H functional combined with the 6-31G(d) basis set. The same theoretical procedure but using the unrestricted formalism was employed for calculations on and ES-$n^+$ (doublet state; *n* ranging from 5 to 11) and ES-$n^{2+}$ (singlet and triplet states; *n* ranging from 5 to 13).

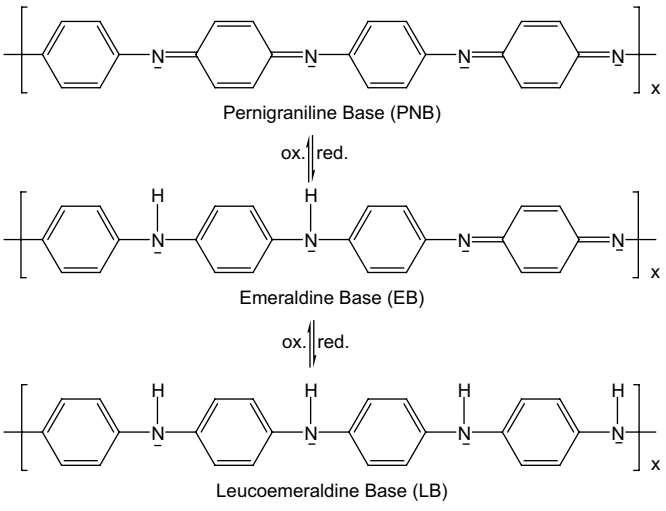


**Scheme 1.**

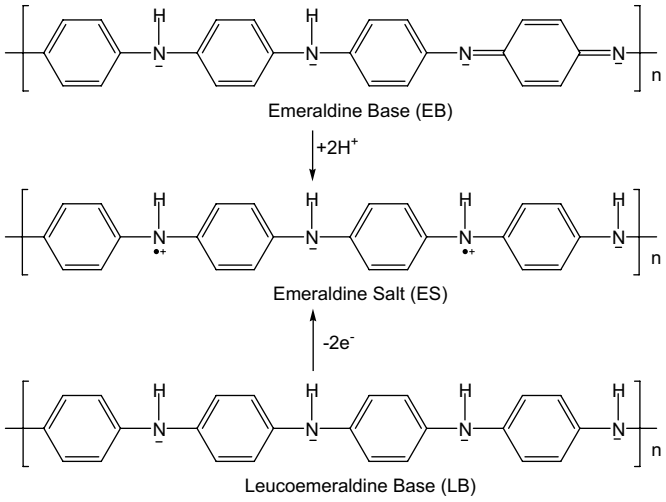


**Scheme 2.**

The $\varepsilon_g$ was approximated as the difference between the highest occupied molecular orbital (HOMO) and the lowest unoccupied molecular orbital (LUMO) energies, *i.e.* $\varepsilon_g = \varepsilon_{LUMO} - \varepsilon_{HOMO}$. It is worth noting that Levy and Nagy evidenced that $\varepsilon_g$ can be rightly approximated as the difference between $\varepsilon_{LUMO}$ and $\varepsilon_{HOMO}$ in DFT calculations [26]. The adiabatic first ionization potential ($IP_{1a}$) was calculated as the energy difference between the optimized structures of the radical cation (ES-$n^+$) and the neutral molecule (LB-$n$), while the adiabatic second ionization potential ($IP_{2a}$) was derived from the energy difference between the optimized structures of the dication in the triplet state (ES-$n^{2+}$(T)) and the radical cation (ES-$n^+$).

## 3. Results and discussion

### 3.1. Choice of the theoretical procedure

Full geometry optimizations of LB-2, PNB-2, ES-$2^+$, ES-$2^{2+}$(S) and ES-$2^{2+}$(T) were performed at the (U)HF/6-31G(d), (U)HF/6-31+G(d,p), (U)HF/cc-pVDZ, (U)HF/cc-pVTZ, (U)B3LYP/6-31G(d), (U)B3LYP/6-31+G(d,p), (U)B3LYP/cc-pVDZ, (U)B3LYP/cc-pVTZ, (U)BH&H/6-31G(d), (U)BH&H/6-31+G(d,p), (U)BH&H/cc-pVDZ, (U)BH&H/cc-pVTZ, (U)MP2/6-31G(d), (U)MP2/6-31+G(d,p) and (U)MP2/cc-pVDZ theoretical levels. The comparison among the results provided by these methods was performed using those obtained at the highest theoretical level, *i.e.* (U)MP2/cc-pVDZ, as the reference.

The optimized structures were analyzed to examine the performance of each method in the description of the following two aspects of PAni: (i) the molecular geometry; and (ii) the relative disposition of adjacent $C_6H_4$ rings. Each of these aspects was represented by a set of well-defined parameters (described below), which vary with the amine or imine nature of the nitrogen and the charge of the system. The performance of the different theoretical procedures against the (U)MP2/cc-pVDZ results was evaluated through the regression coefficient $r$ derived from by a simple linear regression ($y = cx$).

### 3.2. Molecular geometry

The geometric parameters used for this analysis were: the N–C bond lengths ($d_{N-C}$), the angle formed by three consecutive but not directly linked nitrogen atoms ($\angle$N···N···N), the C–N–C bond angle ($\angle$C–N–C) and the C–N–H bond angle (with the obvious exception of PNB-2).

The values of the distances and angles analyzed range from 1.258 to 1.430 Å and 112–138°, respectively, the number of data provided by each theoretical procedure for these statistical analyses being 8 and 15. Inspection of the resulting $r$ values, which are displayed in Table 1, indicates that the intercorrelation between the geometric parameters derived at the MP2/cc-pVDZ level and those calculated using the HF, B3LYP and BH&H methods is similar, even though $r$ is slightly larger for the latter method (especially for angles). On the other hand, the influence of basis set is relatively small independently of the method. Interestingly, the molecular geometries obtained at the B3LYP/cc-pVDZ and BH&H/cc-pVDZ levels are poorly correlated with the MP2/cc-pVDZ ones indicating that this basis set should not be applied within the DFT framework. Obviously the intercorrelation between the results provided by MP2 calculations is excellent in all cases ($r > 0.99$). On the other hand, the global deviation obtained for the HF, B3LYP, BH&H and MP2 geometric parameters is very small in all cases.

### 3.3. Disposition of $C_6H_4$ rings

The geometric parameters used for this analysis were: the dihedral angle associated to the bond between the first ring and the central nitrogen atom ($C_6H_4$–N), the dihedral angle associated to the bond between the same nitrogen atom and the second ring (N–$C_6H_4$) and the dihedral angle formed by the two $C_6H_4$ rings. It should be noted that such three dihedral angles can be defined according to two complementary values. Correlation analyses were performed in all cases considering the higher value in absolute terms.

The resulting statistical parameters are displayed in Table 2. The values of the dihedral angles analyzed range from 108.3° to 176.2°, and the number of data considered for each theoretical procedure is 15. The dependence of the correlation factor on both the theoretical procedure and the basis set is larger for dihedral angles than for distances and angles. The best ab initio and DFT method is the MP2 and BH&H, respectively. Furthermore, the influence of the basis set is very small again. On the other hand, the deviations provided by all the methods and basis sets were small, *i.e.* smaller than 4%.

### 3.4. Selection of the theoretical procedure

Taking into account that oligomers with more than four repeating units are currently untreatable at the MP2 level, we selected the BH&H method to develop the present study. This method combined with the 6-31G(d) basis set, which is the least demanding from a computational point of view, is able to reproduce the molecular geometry including the twisting of the chain backbone. According to these considerations, all the calculations on EB-$n$, LB-$n$, PNB-$n$, ES-$n^+$, ES-$n^{2+}$(S) and ES-$n^{2+}$(T) have performed at the (U)BH&H/6-31G(d) level.

**Table 1**
Regression coefficient ($r$) derived from a regression analysis ($y = cx$) of the geometric parameters (distances and angles) provided by calculations on LB-2, PNB-2, ES-$2^+$, ES-$2^{2+}$(S) and ES-$2^{2+}$(T) using different theoretical procedures and basis sets against those obtained at the highest theoretical level (MP2/cc-pVDZ)

| | 6-31G(d) | 6-31+G(d,p) | cc-pVDZ | cc-pVTZ |
|---|---|---|---|---|
| HF | 0.65 (0.74) | 0.66 (0.74) | 0.67 (0.74) | 0.65 (0.74) |
| B3LYP | 0.60 (0.80) | 0.61 (0.81) | 0.51 (0.76) | 0.62 (0.79) |
| BH&H | 0.65 (0.81) | 0.66 (0.84) | 0.46 (0.82) | 0.69 (0.82) |
| MP2 | 1.00 (0.99) | 0.97 (0.99) | 1.00 (1.00) | – |

For each method: the statistical parameters displayed in top correspond to the analysis of distances (without parenthesis) and angles (in parenthesis).

**Table 2**
Regression coefficient ($r$) derived from a regression analysis ($y = cx$) of the dihedral angles employed to determine the relative disposition of the $C_6H_4$ rings on LB-2, PNB-2, ES-$2^+$, ES-$2^{2+}$(S) and ES-$2^{2+}$(T)

| | 6-31G(d) | 6-31+G(d,p) | cc-pVDZ | cc-pVTZ |
|---|---|---|---|---|
| HF | 0.65 | 0.77 | 0.67 | 0.82 |
| B3LYP | 0.67 | 0.77 | 0.77 | 0.63 |
| BH&H | 0.78 | 0.79 | 0.79 | 0.89 |
| MP2 | 0.99 | 0.98 | 1.00 | – |

Statistical parameters correspond to the values provided by different theoretical procedures and basis sets against those obtained at the highest theoretical level (MP2/cc-pVDZ).

### 3.5. Emeraldine base

Calculations at the BH&H/6-31G(d) level were performed on EB-$n$ with $n = 5$, 7, 9 and 11 considering two different arrangements of the repeating units that involve amine and imine nitrogen atoms, denoted Am and Im, respectively. In the first one the repeating units were distributed according to an alternated sequence, *i.e.* $(Am{-}Im)_{n-1/2}{-}A$, while in the second one they were distributed in two blocks, *i.e.* $(Am)_{n-1/2}{-}(Im)_{n-1/2}{-}A$. In all cases the arrangement with two blocks was the most favored, the destabilization of the alternated sequence growing almost linearly with $n$, *i.e.* the relative energy of the alternated sequence was estimated in 5.5 kcal mol$^{-1}$ per repeating unit. Furthermore, a random distribution of repeating units was also considered for EB-9. This structure was unfavored with respect to that with a distribution in blocks by 25 kcal mol$^{-1}$.

The more relevant geometric parameters of PAni-EB, which are displayed in Fig. 1a, have been obtained by averaging the bond lengths and bond angles obtained for ES-9 and ES-11. As can be seen, the two N–C bond lengths involved in each repeating unit are different independently of the amine or imine nature of the nitrogen atom, such difference being 0.01–0.02 and 0.09–0.10 Å for the Am and Im repeating units, respectively. However, a striking geometrical feature is reflected by the two Im units displayed in Fig. 1a. These Im units present remarkable differences in their N–C bond lengths, while such variations are minimized in the Am ones. This feature is more evident in the backbone bond length patterns (BBLPs). Inspection to the BBLP determined for ES-11, which is provided in Fig. 2a, reveals that the five repeating units contained in the Am-block behave similarly. In contrast consecutive Im repeating units display remarkable differences. Thus, the $C_6H_4$ ring of one of each two consecutive Im units presents a significant degree of quinoid-like structure, whereas the ring of the other shows a benzenoid-like structure similar to that found for the Am repeating units. This pattern is fully consistent with the chemical structure displayed in Scheme 1.

On the other hand, the twisting of the chain backbone was investigated by measuring the dihedral angle defined by neighboring $C_6H_4$ ring. The averaged value of this dihedral was found to be 123° or 120° when the rings are linked to amine or imine nitrogen atoms, respectively. Thus, the deviation from the planarity is very similar for the two types of repeating units. The dihedral angle was slightly smaller (117°) when the rings belong to different types of repeating units, *i.e.* Am and Im. However, the influence of

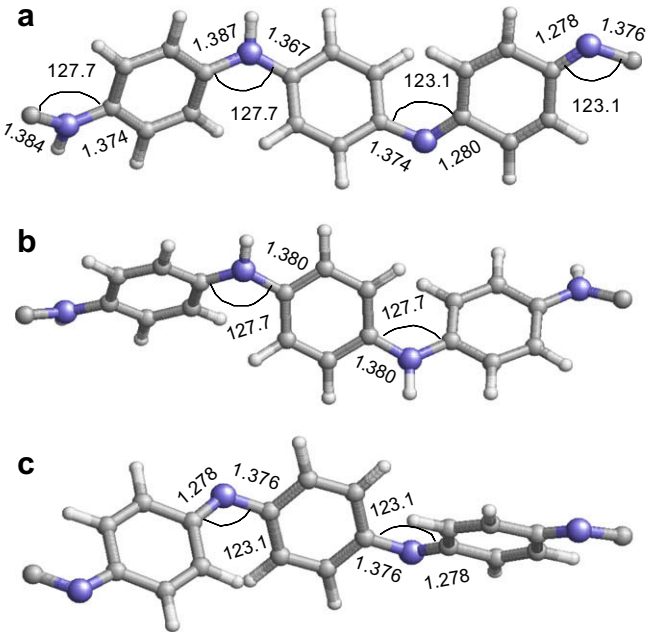


**Fig. 1.** Averaged geometric parameters (bond lengths and bond angles in Å and °, respectively) obtained for (a) PAni-ES, (b) PAni-LB and (c) PAni-PNB.

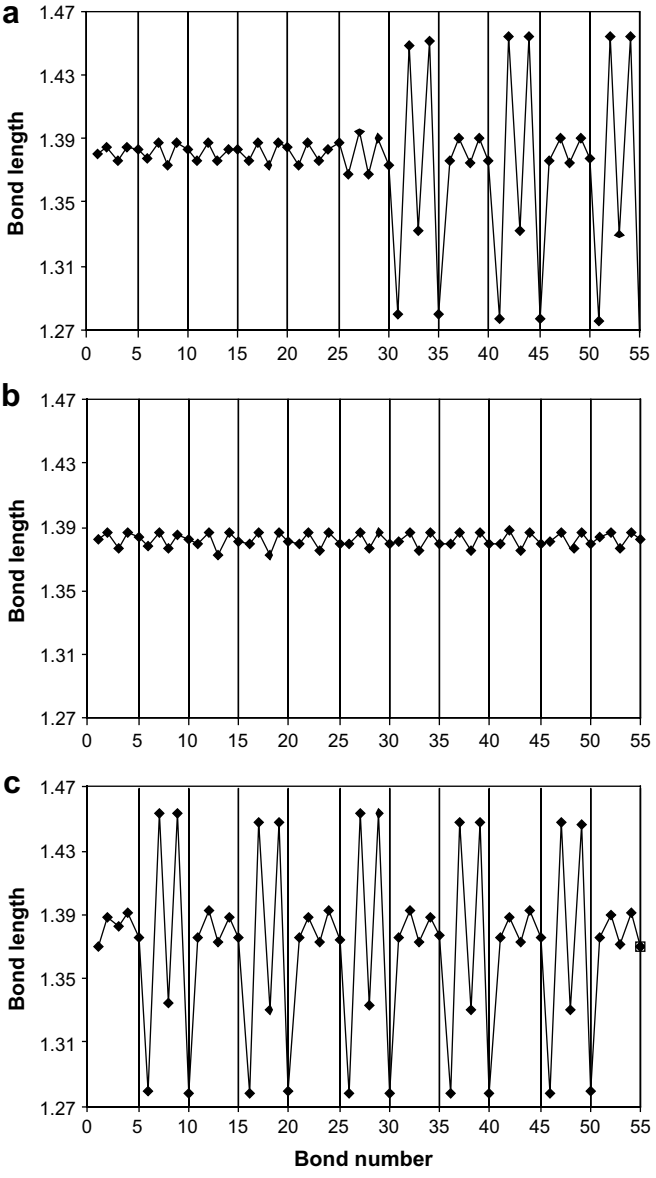


**Fig. 2.** Backbone bond length patterns obtained for (a) EB-11, (b) LB-11 and (c) PNB-11. Repeating units are separated by vertical thin lines.

this reduction in the regular twisting of the molecular chain is almost negligible.

The $\varepsilon_g$ calculated for the optimized oligomers with a distribution in blocks revealed a reduction from 4.10 to 3.83 eV when $n$ increases from 5 to 11. Fig. 3 shows a perfect linear behaviour (correlation coefficient $r > 0.99$) for the variation of the calculated $\varepsilon_g$ with the inverse chain length ($1/n$). A linear regression analysis, which is also displayed in Fig. 3, allowed extrapolate a $\varepsilon_g$ of 3.60 eV for an infinite chain of Pani-EB. This value is in good agreement with accurate nanoscale measurements recently obtained using current-sensing atomic force microscopy and atomic force microscopy current image tunneling spectroscopy, which were all higher than 3.8 eV [27].

### 3.6. Leucoemeraldine base

Geometry optimizations of LB-$n$ oligoanilines with $n = 5$, 7, 9 and 11, in which all the repeating units involve amine nitrogen, were used to derive the geometric parameters displayed in Fig. 1b. Interestingly, the averaged bond lengths and bond angles around the nitrogen atom led to a symmetric geometry, which was not found in the Am repeating units of EB-$n$. This result evidences that in the latter oligoanilines the block formed by Im units affects the geometric parameters of the block formed by Am units, even though that the influence of Am units in the block formed by Im units is negligible (see below). This feature is also illustrated by the BBLP showed in Fig. 2b, which reflects the benzenoid-like structure of the $C_6H_4$ rings in LB-11. On the other hand, the twisting of the chain backbone was almost identical to that described for PAni-EB.

The $\varepsilon_g$ values obtained for LB-$n$ ranged from 6.06 ($n = 5$) to 5.83 eV ($n = 11$) indicating that the gap grows when the structure of oligomers change from the half oxidized form to the fully reduced form. This is because the $C_6H_4$ rings are linked to saturated amine nitrogen atoms, which inhibit conjugation. The $\varepsilon_g$ extrapolated for an infinite polymer chain of PAni-LB is 5.64 eV (Fig. 3). This value is larger than those determined experimentally, *i.e.* the maximum in the $\pi$–$\pi^*$ optical absorption spectrum in PAni-LB was found to be 3.6 eV in *N*-methylpyrrolidine solution and 3.8 eV in thin films [28–31], although very close to other theoretical predictions derived from ab initio quantum mechanical methods, *i.e.* 4.29–5.08 eV [32]. The general lack of agreement between theoretical and experimental values suggests that PAni-LB films involve external components (for example, water taken from humid environments), which affects the measures and are not considered in theoretical estimations.

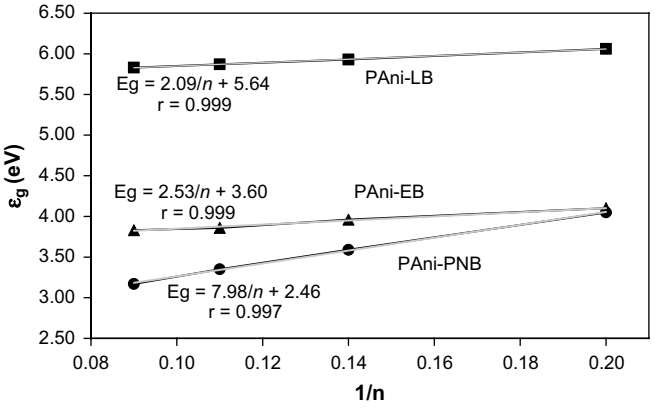


**Fig. 3.** Variation of $\varepsilon_g$ (in eV) against $1/n$, where $n$ is the number of repeating units, for PAni-EB, PAni-LB and PAni-PNB. The grey lines correspond to the linear regressions used to obtain the $\varepsilon_g$ for infinite chain systems.

### 3.7. Pernigraniline base

Calculations on PNB-$n$ with $n = 5$, 7, 9 and 11 evidenced that our previous observations on the Im-containing block of EB-$n$ oligoanilines are retained when the latter systems are fully oxidized. Fig. 2c shows the BBLP, which reflect that, as expected, consecutive Im repeating units present a different structure. Thus, the $C_6H_4$ rings with quinoid-like and benzenoid-like structures are alternated. The geometric parameters averaged for the Im units with rings adopting quinoid-like and benzenoid-like structures are displayed in Fig. 1c.

The values of $\varepsilon_g$ calculated for PNB-$n$ ranged from 4.05 ($n = 5$) to 3.16 eV ($n = 11$), the value extrapolated for an infinite polymer chain of PAni-PNB being 2.46 eV (Fig. 3). These calculations predict satisfactorily the reduction detected in the $\varepsilon_g$ when PAni-ES is submitted to a full oxidation process (Scheme 1), even though our theoretical estimation is slightly larger than that experimental measures, *i.e.* 1.7–2.3 eV [33–37]. The considerable reduction observed in the band gap of PNB-$n$ when compared to EB-$n$ and LB-$n$ is due to the conjugation of the $C_6H_4$ rings through the imine linkages, which in the former oligoanilines extend through the whole chain.

### 3.8. Emeraldine salt (cationic form)

Calculations on ES-$n^+$ with $n$ ranging from 5 to 11 were performed at the UBH&H/6-31+G(d,p) level. The BBLP determined for ES-$11^+$ is represented in Fig. 4a, the BBLP previously determined for LB-11 being also displayed for comparison. As can be seen, the positive charge basically affects the geometry of the five central repeating units of ES-$11^+$. Fig. 4a clearly shows the evolution of the

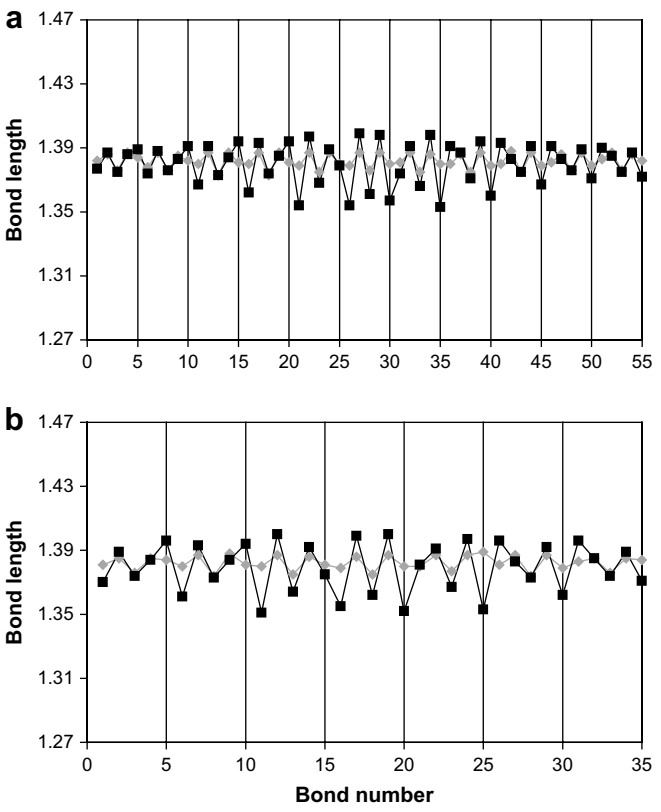


**Fig. 4.** Backbone bond length patterns obtained for (a) ES$^+$-11 (black) and LB-11 (grey); and (b) ES-$7^+$ (black) and LB-7 (grey). Repeating units are separated by vertical thin lines.

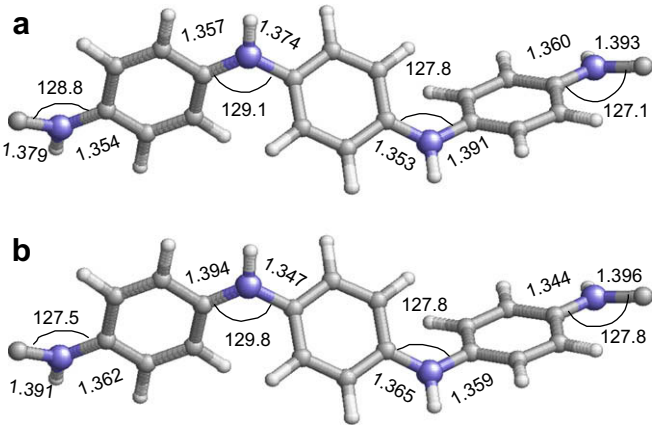


**Fig. 5.** Geometric parameters (bond lengths and bond angles in Å and degrees, respectively) obtained for (a) ES-11$^{+}$ (central repeating units) and (b) ES-11$^{2+}$(T) (repeating units located at the chain end).

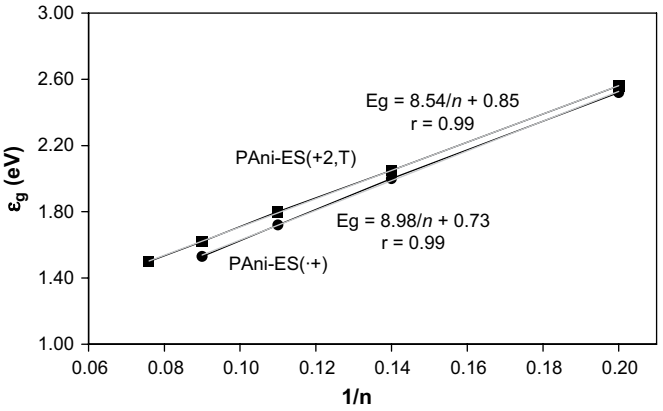


**Fig. 7.** Variation of $\varepsilon_g$ (in eV) against $1/n$, where $n$ is the number of repeating units, for ES-$n^{+}$ and ES-$n^{2+}$ oligomers. The grey lines correspond to the linear regressions used to obtain the $\varepsilon_g$ for infinite chain systems.

$C_6H_4$ rings towards the quinoid-like form, the bond that connects such rings with the nitrogen atoms being also affected by the positive charge. The latter feature is reflected in Fig. 5a, which displays the geometric parameters obtained for the central-repeating units of ES-11$^{+}$. A similar conclusion is reached from comparison of the BBLPs obtained for ES-7$^{+}$ and LB-7 (Fig. 4b). In this case the geometrical distortions induced by the positive charge affects to almost the whole molecule, the $C_6H_4$ ring of the repeating units located at the ends being the only able to retain the benzenoid-like structure, *i.e.* the quinoid form extends along the five central repeating unit of ES-7$^{+}$. On the other hand, analysis of the results obtained for ES-5$^{+}$ and ES-9$^{+}$ (data not shown) indicates that in the former the charge extends along the whole molecule, while in the latter geometrical distortions are similar to those described for ES-7$^{+}$ and ES-11$^{+}$, *i.e.* the quinoid-like form is concentrated in the five central rings. These results reflect that the minimum number of repeating units required to describe the extension of cationic defects in PAni-ES is 7. It should be noted that previous results on thiophene-containing oligomers concluded that oligomers with around 10 monomeric units are desirable to provide a realistic description of the cationic and dicationic p-doped polythiophenes [3,38,39]. On the other hand, the average value of the dihedral angle defined by neighboring $C_6H_4$ rings (124°) is very similar to that found for PAni-EB. However, a detailed analysis reveals that the value of this structural parameter is larger for the central repeating units (130°), in which the positive charge is localized, than for those of the ends (116°). Accordingly, the introduction of positive charges produces small structural distortions in the twisting of the backbone.

The Mulliken population analysis was used to calculate the distribution of charges along the repeating units of ES-11$^{+}$ oligomers (Fig. 6). On the other hand, to clarify the charge transport mechanism, we also evaluated the spin density per repeating unit in the same oligomer (Fig. 6). Thus, as can be seen, both the charges and the spin densities are moved from the chain ends to the middle. Furthermore, the distribution of both the charges and the spin densities fully support the interpretation provided above of the BBLP, *i.e.* the charges and spin densities are basically localized in five central repeating units.

The $\varepsilon_g$ predicted for ES-$n^{+}$ ranged from 2.52 ($n=5$) to 1.53 eV ($n=11$), which represents an important reduction with respect to the values obtained for EB-$n$, LB-$n$ and PNB-$n$. Fig. 7 plots the calculated $\varepsilon_g$ values against the inverse chain length, the extrapolation to an infinite polymer chain being 0.73 eV. Although this estimation is consistent with the band gap reduction observed when undoped PAni transforms into PAni-ES, it is underestimated with respect to the value experimentally measured, *i.e.* absorption spectra for PAni-ES showed a $\varepsilon_g$ of 1.5 eV [30,40,41].

On the other hand, Fig. 8 represents the variation of the adiabatic first ionization potential ($IP_{1a}$) against the inverse of the chain length. As can be seen, the dependence of $IP_{1a}$ on the chain length is very small, the calculated values ranging from 5.19 ($n=5$) to 4.88 eV ($n=11$). The $IP_{1a}$ extrapolated for an infinite polymer chain is 4.62 eV. This value is similar to those recently calculated for

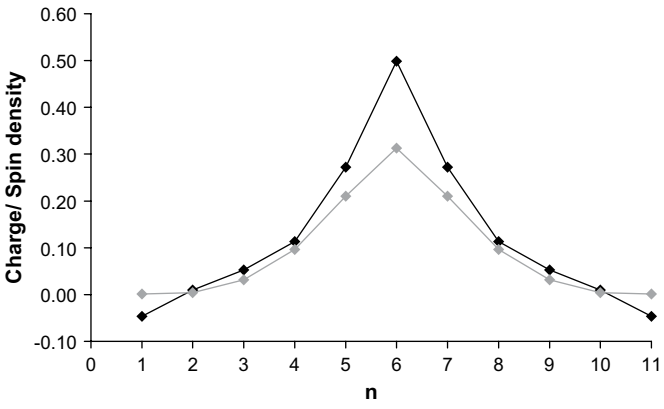


**Fig. 6.** Mulliken charge (black) and spin density (grey) per repeating unit calculated for ES-11$^{+}$. The charges and spin densities of the $NH_2$ blocking groups are not displayed.

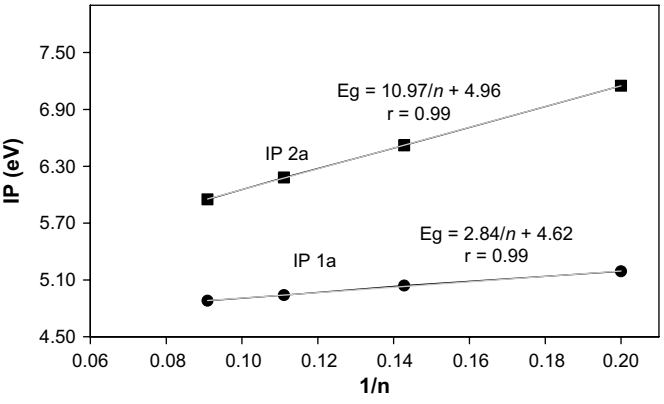


**Fig. 8.** Variation of $IP_{1a}$ and $IP_{2a}$ (both in eV) against $1/n$, where $n$ is the number of repeating units. The procedure used to estimate IP is indicated in the Section 2. The grey lines correspond to the linear regressions used to obtain the IPs for infinite chain systems.

polythiophene and polyselenophene (4.60 and 4.56 eV, respectively) using the B3LYP/6-31G(d) method [42].

### 3.9. Emeraldine salt (dicationic form)

The optimized geometries and energies of ES-$n^{2+}$(S) and ES-$n^{2+}$(T) with $n = 5$, 7, 9, 11 and 13 have been analyzed. The two electronic states were studied because oxidized oligomers carrying two charges may have either a singlet or a triplet ground state depending on their radical nature. The spin contamination was very low in all cases, that is, the largest $S^2$ value found for the singlet and triplet states was 1.06 and 2.06, respectively.

Results show that the singlet ground state is the most stable for small oligomers ($n = 5$ and 7), even though the stability of the triplet increases with the chain length. The most striking feature if that for $n = 9$, 11 and 13 the two electronic states become isoenergetic. This unexpected result clearly contrasts with those obtained for thiophene-, pyrrole-, phosphole- and 3,4-ethylenedioxythiophene-containing oligomers [3,25]. In all cases it was found that small oligomers prefer the singlet ground state but the diradical electronic structure with two unpaired electrons is favored for oligomers with eight or more repeating units. A detailed analysis of the results (BBLP, distribution of charges and spin densities) on oligomers with $n = 9$, 11 and 13 indicates that the BH&H functional is not able to describe the singlet ground state of dicationic oligomers after a given size. This method provides an over-delocalization of the charges, and calculations on the singlet ground state converge into the triplet ground state solution.

The BBLP of ES-11$^{2+}$(T) is represented in Fig. 9a, that of LB-11 being displayed for comparison. As can be seen, the three central rings of the charged oligomer show a benzenoid character, whereas the structure becomes more quinoid-like towards the molecular

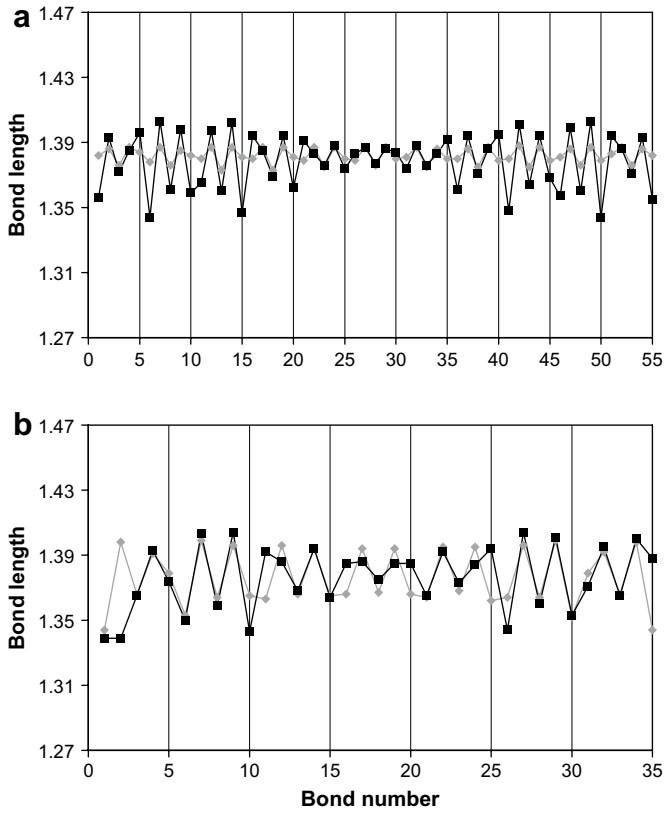


**Fig. 9.** Backbone bond length patterns obtained for (a) ES$^{2+}$-11 (black) and LB-11 (grey); and (b) ES-7$^{2+}$(T) (black) and ES-7$^{2+}$(S) (grey). Repeating units are separated by vertical thin lines.

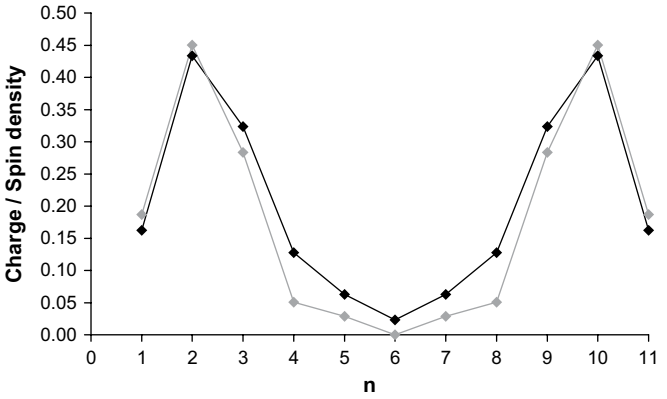


**Fig. 10.** Mulliken charge (black) and spin density (grey) per repeating unit calculated for ES-11$^{2+}$(T). The charges and spin densities of the $NH_2$ blocking groups are not displayed.

ends with exception of the terminal rings. Thus, the structure of doubly oxidized oligomers in the triplet ground state looks like two quinoid-like parts separated by aromatic rings in the middle of the chain. Fig. 9b, which compares the BBLPs obtained for ES-7$^{2+}$(T) and ES-7$^{2+}$(S), indicates that the biradical dication nature of the triplet state is similar to that showed above for ES-11$^{2+}$(T). In contrast, the deformation associated to the formation a bipolaron is wrongly described for ES-7$^{2+}$(S). Thus, the BBLP showed in Fig. 9b for the latter oligomer differs significantly from that previously calculated for oligomers of thiophene and pyrrole with a similar size [3]. The BH&H functional describes the two positive charges as uniformly distributed along the chain rather than as a bipolaron, this deficiency being previously reported for other DFT methods [43,44]. Accordingly, we concluded that the results provided by UBH&H/6-31G(d) calculations on ES-$n^{2+}$(S) are not representative independently of the value of $n$.

On the other hand, the distribution of charges and spin densities along the monomers in ES-11$^{2+}$(T) (Fig. 10) shows that both are mainly located at the chain ends, which is in good agreement with the BBLP displayed in Fig. 9a. The geometric parameters averaged for the repeating units located at the chain ends are displayed in Fig. 5b. As can be seen, the influence of the positive charge is slightly more marked in the C–N bond lengths of ES-11$^{2+}$(T) than in ES-11$^{+}$(Fig. 5a). The dihedral angle defined by the neighboring $C_6H_4$ rings is 131° for the repeating units located at the ends, *i.e.* charged fragment of the oligomer chain, and 117° for the repeating units with a benzonoid-like structure. These values are very similar to those obtained for ES-$n^{+}$ indicating the twisting undergoes perturbations in the charged segments of the polymer chain. Fig. 7 represents the variation of $\varepsilon_g$ against $1/n$ for ES-$n^{2+}$(T). The values ranged from 2.56 ($n = 5$) to 1.50 eV ($n = 13$), the value obtained for an infinite polymer chain being 0.73 eV. This estimation, which is close to that derived from the ES-$n^{+}$ oligomers, is underestimated with respect to the value experimentally determined for PAni-ES ($\varepsilon_g = 1.5$ eV) [30,40,41]. Finally, the variation of the adiabatic second ionization potential ($IP_{2a}$) with the inverse of the chain length is included in Fig. 8. As can be seen, the $IP_{2a}$ range from 7.15 ($n = 5$) to 5.95 eV ($n = 11$), the value extrapolated for an infinite polymer chain being 4.96 eV. This value is only 0.34 eV higher than that obtained for $IP_{1a}$ indicating that the conducting model based on pair of polarons is highly favored in PAni-ES.

## 4. Conclusions

Quantum mechanical calculations have been applied to perform a systematic study on the different undoped (PNB, EB and LB) and p-

doped (ES) forms of PAni. From a theoretical point of view, calculations on small model compounds allow us to conclude that the (U)BH&H/6-31G(d) level of calculation is accurate enough to describe satisfactorily the main structural characteristics of this family of compounds. Accordingly, this theoretical method has been used to analyze the structural (parameters that define the backbone geometry) and electronic (IP, $\varepsilon_g$, spin and charge distribution) properties of long oligoanilines, as well as the stability of different isomers. Results indicate that some properties of the infinite polymer chains can be obtained by extrapolation. From an applied point of view, the results obtained agree with the available experimental data and, in consequence, can be used to understand the main geometric and electronic properties of the different PAni forms. In particular, it is worth noting that PAni-EB shows a clear preference for a distribution in blocks of the repeating units containing the amine and imine nitrogen atoms. Like PAni-EB, the properties of the PAni-LB and PAni-PNB have been rationalized according to their electron distribution and optimized geometries. Calculations on PAni-ES (cationic and dicationic oligoanilines) are of special interest because of their low $\varepsilon_g$ value. The analysis of the monocationic form reveals that the doping defect is concentrated in the five central rings of the chain, which adopt a quinoid-like structure and concentrate the charge and the spin density, this number of monomeric units being considerable lower than that previously determined for other conducting polymers. On the other hand, examination of the geometry, charge distribution and spin densities of the dicationic oligomers suggests that this p-doped compound can be described by a triplet electronic state with two separated polarons.

## Acknowledgements

This work was supported by MEC and FEDER funds with Grants MAT2006-04029 and PHB2007-0038-PC, as well as by CAPES-MECD International Cooperation Program from Brazilian and Spanish Education Ministries. Gratitude is expressed to the Centre de Supercomputació de Catalunya (CESCA) and to the Universitat de Lleida for computational facilities.

## References

[1] Brédas JL. Adv Mater 1995;7:263.
[2] Brédas JL, Cornil J, Beljonne D, Dos Santos DA, Shuai Z. Acc Chem Res 1999;32:267.
[3] Casanovas J, Alemán C. J Phys Chem C 2007;111:4823.
[4] Zade SS, Bendikov M. Org Lett 2006;8:5243.
[5] Hutchison GR, Ratnet MA, Marks TJ. J Am Chem Soc 2005;127:2339.
[6] Hutchison GR, Ratnet MA, Marks TJ. J Phys Chem B 2005;109:3126.
[7] Casanovas J, Zanuy D, Alemán C. Polymer 2005;46:9452.
[8] Bertran O, Pfeiffer P, Torras J, Armelin E, Estrany F, Alemán C. Polymer 2007;48:6955.
[9] Know O, McKee ML. J Phys Chem B 2000;104:1686.
[10] Cavazzoni C, Colle R, Farchioni R, Grosso G. Phys Rev B 2002;66:165110.
[11] Zhekova H, Tadjer A, Ivanova A, Petrova J, Gospodinova N. Int J Quantum Chem 2007;107:1688.
[12] Lim SL, Tan KL, Kang ET, Chin WS. J Chem Phys 2000;112:10648.
[13] Foreman JP, Monkman P. J Phys Chem A 2003;107:7604.
[14] Varela-Alvarez A, Sordo JA, Scusseria GE. J Am Chem Soc 2005;127:11318.
[15] Yang G, Hou W, Feng XO, Jiang X, Guo J. Int J Quantum Chem 2008;108:1155.
[16] Frisch MJ, Trucks GW, Schlegel HB, Scusseria GE, Robb MA, Cheeseman JR, et al. Gaussian 03: Revision B.02. Pittsburgh, PA: Gaussian, Inc.; 2003.
[17] Møller C, Plesset M. Phys Rev 1934;46:618.
[18] Becke AD. J Chem Phys 1993;98:1372.
[19] Lee C, Yang W, Parr RG. Phys Rev B 1993;37:785.
[20] Hariharan PC, Pople JA. Theor Chim Acta 1973;28:213.
[21] Petersson GA, Al-Laham MA. J Chem Phys 1994;94:6081.
[22] Woon DE, Dunning Jr TH. J Chem Phys 1993;98:1358.
[23] Kendall RA, Dunning Jr TH, Harrison RJ. J Chem Phys 1992;96:6796.
[24] Waller MP, Robertazzi A, Platts JA, Hibss DE, Williams PA. J Comput Chem 2006;27:491.
[25] Geskin VM, Brédas JL. Chem Phys Chem 2003;4:498.
[26] Levy M, Nagy A. Phys Rev A 1999;59:1687.
[27] Wu CG, Chang SS. J Phys Chem B 2005;109:825.
[28] McCall RP, Ginder JM, Leng JM, Yee HJ, Manohar SK, Masters JG, et al. J Phys Rev B 1990;41:5202.
[29] Cao Y, Smith P, Heeger AJ. Synth Met 1989;32:263.
[30] Cully S, Petty MC, Monkman AP. Synth Met 1993;55–57:183.
[31] D'Aprano G, Leclerc M, Zotti G. Synth Met 1996;82:59.
[32] Ho C, Kertesz M. Macromolecules 1997;30:620.
[33] Cao Y. Synth Met 1990;35:319.
[34] Leng JM, Ginder JM, McCall RP, Ye HJ, Epstein AJ, Sun Y, et al. Synth Met 1991;41–43:1311.
[35] Osaheni JA, Jenekhe SA, Vanherzeele H, Meth JS, Sun Y, MacDiarmid AG. J Phys Chem 1992;96:2830.
[36] Leng JM, McCall RP, Cromack KR, Sun Y, Manohar SK, MacDiarmid AG, et al. Phys Rev B 1993;48:15719.
[37] Coplin KA, Jasty S, Long SM, Manohar SK, Sun Y, MacDiarmid AG, et al. Phys Rev Lett 1994;72:3206.
[38] Ehrendorfer Ch, Karpfen A. J Phys Chem 1994;98:7492.
[39] Ire S, Lischka H. J Chem Phys 1995;103:1508.
[40] Stafström S, Brédas JL, Epstein AJ, Woo HS, Tanner DB, Huang WS, et al. Phys Rev Lett 1987;59:1464.
[41] Liu W, Kumar J, Tripathy S, Senecal KJ, Samuelson L. J Am Chem Soc 1999;121:71.
[42] Zade SS, Bendikov M. Chem Eur J 2008;14:6734.
[43] Moro G, Scalmani G, Cosentino U, Pitea D. Synth Met 1998;92:69.
[44] Dkhissi A, Beljonne D, Lazzaroni R, Louwet F, Groenendaal L, Brédas JL. Int J Quantum Chem 2003;91:517.